Overland flow during a storm event strongly affects stream water chemistry and bacterial community structure

Huong T. Le, Thomas Pommier, Olivier Ribolzi, Bounsamay Soulileuth, Sylvain Huon, Norbert Silvera, Emma Rochelle-Newall

▶ **To cite this version:**

Huong T. Le, Thomas Pommier, Olivier Ribolzi, Bounsamay Soulileuth, Sylvain Huon, et al.. Overland flow during a storm event strongly affects stream water chemistry and bacterial community structure. Aquatic Sciences - Research Across Boundaries, 2022, 84 (1), pp.7. 10.1007/s00027-021-00839-y . hal-04205924

HAL Id: hal-04205924
https://hal.inrae.fr/hal-04205924

Submitted on 13 Sep 2023

HAL is a multi-disciplinary open access archive for the deposit and dissemination of scientific research documents, whether they are published or not. The documents may come from teaching and research institutions in France or abroad, or from public or private research centers.

L'archive ouverte pluridisciplinaire **HAL**, est destinée au dépôt et à la diffusion de documents scientifiques de niveau recherche, publiés ou non, émanant des établissements d'enseignement et de recherche français ou étrangers, des laboratoires publics ou privés.

Aquatic Sciences (2022) 84:7
https://doi.org/10.1007/s00027-021-00839-y

Aquatic Sciences

RESEARCH ARTICLE

Overland flow during a storm event strongly affects stream water chemistry and bacterial community structure

Huong T. Le[1,2,3] · Thomas Pommier[1] · Olivier Ribolzi[4] · Bounsamay Soulileuth[5] · Sylvain Huon[3] · Norbert Silvera[5,6] · Emma Rochelle-Newall[3]

Received: 28 January 2021 / Accepted: 19 November 2021
© The Author(s), under exclusive licence to Springer Nature Switzerland AG 2021

Abstract

As flood events are expected to become more frequent due to climate change, investigating how overland flow exports terrestrial nutrients, carbon and living organisms into aquatic systems is essential for understanding both soil and stream ecosystem status. Here we assessed how dissolved organic carbon (DOC), total suspended sediments (TSS), and stream bacterial diversity responded to stream discharge and overland flow during stormflow in a tropical catchment. A higher humification index and a decreasing ratio of allochthonous to autochthonous DOC indicated that DOC from soils was exported to stream during the flood. The $\delta^{13}C$ and $\delta^{15}N$ of particulate matter was indicative of a source in the cultivated areas of the upper catchment and of subsurface soils (stream banks and gullies) in the downstream section. Bacterial richness of particle-attached (PA) and the free-living (FL) fractions increased with the flood progression in the upstream section. Moreover, the community structure of the PA fraction in the stream was more similar to that of overland flow than was the FL fraction. This suggests that the soil PA bacterial community was washed-out with overland flow during the flood recession. The relative contribution of sources and the composition of TSS, rather than hydrological regime, significantly drove the composition of bacterial community. In conclusion, our results emphasize that overland flow during a flood event strongly influences the structure of stream bacterial communities further underlining the biological connectivity between terrestrial runoff and stream flow.

Keywords DOC · CDOM · Lao PDR (Laos) · Southeast Asia · Land degradation · Sustainability

Introduction

The increase in frequency and intensity in flash flood events due to global warming has caused alarm due to their impact on soil erosion and stream ecosystem functioning (Trenberth 2011; Marengo and Espinoza 2016; Polade et al. 2017; Talbot et al. 2018; Eccles et al. 2019). Flash floods in streams are generated by a combination of high rainfall rate with rapid and efficient runoff production. Flash floods take place rapidly within a few hours of a rainfall event and have relatively high peak discharges that are determined by the dynamic of rainfall variability and its complex interaction with basin characteristics (Syed et al. 2003). The amount and timing of overland flow occurring during a flood event are regulated by basin shape and size (Syed et al. 2003), soil moisture (Ali and Roy 2010), surface roughness and crusting as well as vegetation cover (Valentin and Bresson 1992; Poeppl et al. 2012; Trevisani and Cavalli 2016).

Overland flow during floods redistributes material across the landscape mosaic when water, soil, nutrients

✉ Emma Rochelle-Newall
Emma.Rochelle-newall@ird.fr

1 CNRS, INRAE, VetAgro Sup, UMR Ecologie Microbienne, Univ Lyon, Université Claude Bernard Lyon 1, 69622 Villeurbanne, France

2 Institute of Environmental Technology, Vietnam Academy of Science and Technology, Hanoi, Vietnam

3 Sorbonne Université, Univ Paris Est Creteil, IRD, CNRS, INRAE, Institute of Ecology and Environmental Sciences of Paris (iEES-Paris), 4 Place Jussieu, 75005 Paris, France

4 Géosciences Environnement Toulouse (GET), UMR 5563 (CNRS UPS IRD), 14 Avenue Edouard Belin, 31400 Toulouse, France

5 IRD, Ban Sisangvone, BP 5992, Vientiane, Laos

6 Centre IRD Île-de-France, Sorbonne Université, Univ Paris Est Creteil, IRD, CNRS, INRAE, Institute of Ecology and Environmental Sciences of Paris (iEES-Paris), 32 Avenue Henri Varagnat, 93143 Bondy, France

Published online: 03 December 2021

and organic material are transferred across the landscape (Belnap et al. 2005; Chaplot et al. 2005). The mobilization of nutrients and organic matter may increase with soil erosion intensity and suspended matter transport during flooding, and land use is known to affect nutrient loading to downstream ecosystems (Lamers et al. 2006; Banach et al. 2009; Maiga-Yaleu et al. 2013; Gourdin et al. 2014a). Such transfer consequently impacts stream biology, especially its microbial component that can rapidly respond to environmental variations (Zeglin 2015; Kan 2018). Stream microbial communities are shaped by different processes relating to local environmental factors or to dispersal mechanisms (Lindström and Langenheder 2012) and the bacterial community transported from soils into streams can easily adapt and persist in new habitats due to frequent and high dispersal rates (Adams et al. 2014).

Dissolved organic carbon (DOC) from terrestrial sources influences stream microbial activity, growth and bacterial composition and diversity through selective local processes (Carvalho et al. 2003; Carney et al. 2015). The quantity and quality of allochthonous DOC drained from different soils and flushed into a stream play a critical role for aquatic bacterial growth (Kirchman et al. 2004; Agren et al. 2008). However, to our knowledge, the impact of overland flow, including the associated bacterial community, on shifting stream bacterial diversity and structure during a tropical flood event remains little studied, especially in tropical regions where flash floods are particularly frequent.

The Houay Pano catchment, Lao PDR is characteristic of tropical mountainous catchments in Southeast Asia in that it experiences heavy rainfall during the summer monsoon. Recent studies focused on suspended sediment transport and *Escherichia coli* (*E. coli*) numbers during rainy season storm flow events in this catchment have emphasized the influence of overland flow in the transfer of *E. coli* from the soil surface into the stream (Causse et al. 2015; Mügler et al. 2021; Nakhle et al. 2021). Ribolzi et al. (2016) found that a small percentage of overland flow, i.e. one tenth of the total flood volume in the flood event, was responsible for more than two thirds of the downstream transfer of *E. coli* in this catchment. Furthermore, other work has shown that the percentage of overland flow in stream water is strong predictor of stream *E. coli* concentrations (Boithias et al. 2021a). These results raise the question of whether overland flow originating from the surface of upland soils is a major factor controlling stream bacterial diversity and structure including particle attached (PA) and free living (FL) bacterial fractions at the scale of the flood. We therefore hypothesized that overland flow associated to a flood event would strongly structure PA and FL bacterial fractions and that proportions of the different fractions would follow flood hydrology, with the strongest influence observed at peak flood when overland flow was highest.

Materials and methods

Study sites

The study site is located 10 km south of Luang Prabang in northern Laos (Fig. 1). It is a sub-catchment of the Houay Xon River, a tributary of the Mekong River. The climate pattern is that of a tropical climate with summer monsoon characterized by a rainy season from mid-May to mid-October and the dry season from November to March. The average annual rainfall is ca. 1366 mm with 77% occurring during the rainy season. The watershed is characterized by intense, monsoonal rain events of which around 20–30 generate flood events annually. During these storms, rainfall reaches intensities of up to 100 mm h^{-1} (over a time step of 6 min), similar to that commonly observed in other tropical systems (Richter et al. 2016).

The catchment is part of the M-TROPICS network of instrumented catchments (Boithias et al. 2021b). Three hydrometric stations that allowed continuous monitoring of stream discharge and water sampling at the outlet of three nested catchments were selected for this work (Fig. 1). The Overland flow station (S8) is located upstream of the Intermediate station (S4), both are within the Houay Pano catchment. The Downstream station (S10) is located downstream and is within the Houay Xon catchment, of which Houay Pano is a sub-catchment. During flood events, the Overland flow station drains ephemeral overland flow (Gourdin et al. 2015) from a small hollow (0.01 km^2). The Intermediate and the Downstream gauging stations, corresponding to a drainage area of 0.62 and 11.6 km^2, respectively, monitor the permanent flow of the main stream during baseflow (groundwater contribution only) and stormflow (mixture of groundwater with overland flow) periods (Ribolzi et al. 2018). At the time of the study, the study site was covered by forests (56% of the total surface area), teak plantations (15%) and croplands (23%) (Fig. 1).

Water sampling and hydrological measurement

Water sampling took place during a flood event on June 16th, 2014. Water samples were collected in new, double rinsed, 19 L plastic drinking water carboys by an automatic sampler (Automatic Pumping Type Sediment Sampler, ICRISAT) at each station (Overland (S8), Intermediate (S4) and Downstream (S10) (Fig. 1) Samples were collected every 2 cm during the flood stage and every 4 cm during the recession stage. Ten samples from the Intermediate station, six samples from the Downstream station and two additional samples at the Overland station (at the

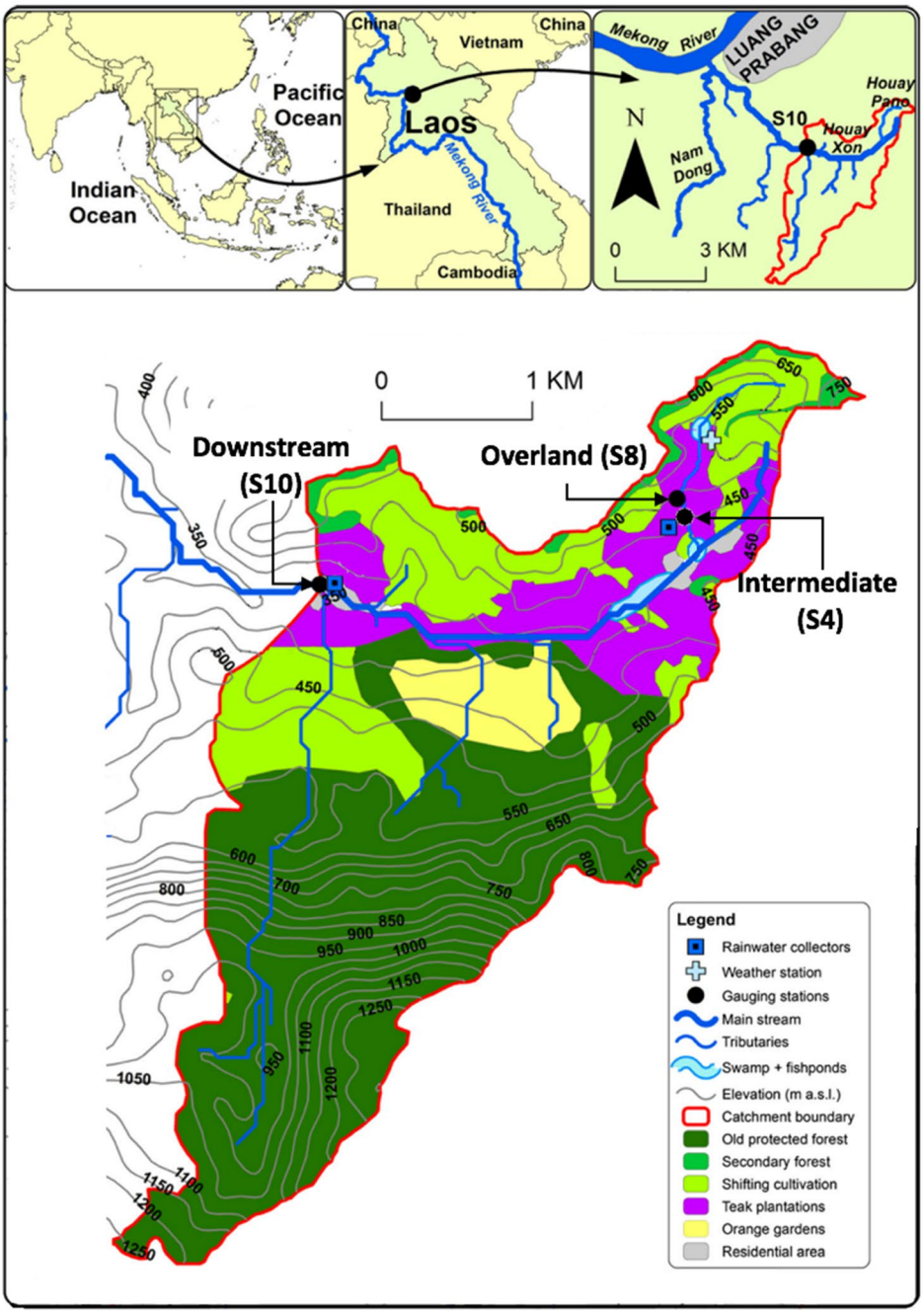

Fig. 1 Location of study and sampling sites: in stream monitoring stations (Intermediate station, S4), the Downstream station, S10) and direct source sample locations and hillslope in situ sediment source sampling station (Overland station, S8) (overland flow) (Evrard et al. 2016)

beginning and the end of the flood) were collected over the course of flood. We estimate that a maximum delay of 2 h occurred between the end of the flood and the start of sample treatment in the laboratory.

Hydrological measurements were made at the Intermediate and Downstream stations. Rainwater intensity was measured (with a 1-min time step) using an automatic rain gauge. Stream discharge was measured at the catchment outlets (Intermediate and Downstream) using an automated water level recording station (OTT, Thalimedes/SE200). Water electrical conductivity (EC) normalized to 25 °C was measured for each sample with an YSI 556 probe.

EC-based hydrograph separation

To separate overland flow and groundwater flow during the flood event, a tracer-based approach was used with a simple mixing model with two reservoirs and EC as a tracer (Ribolzi et al. 2016). It is described by the following equations:

$$Q_{sw} = Q_{of} + Q_{gw},$$

$$Q_{sw}EC_{sw} = Q_{of}EC_{of} + Q_{gw}EC_{gw},$$

where Q_{sw} represents the instantaneous stream water discharge at the catchment outlet, Q_{of}, the instantaneous discharge of overland flow and Q_{gw}, the instantaneous discharge of groundwater (expressed in L s^{-1}). EC_{SW} is the instantaneous EC measured in the stream. EC_{of} is the average value for overland flow during the storm event. EC_{of} was measured on samples of overland flow that were collected from the soil surface on hillslopes draining to the stream during the rainfall event (Patin et al. 2018). Since groundwater feeds the stream during inter-stormflow periods (Ribolzi et al. 1997, 2018), EC of groundwater (EC_{gw}) was approximated from stream measurements carried out prior to the storm event at the catchment outlets (Intermediate and Downstream).

Measurement of DOC, CDOM and TSS

The Intermediate and Downstream stations were used to monitor DOC, CDOM and TSS variations during the flood event. A subsample of 200 mL of each sample was filtered through 0.7 µm nominal porosity Whatman GF/F glass fiber filters to remove particles. Sample filtration for all of the samples took a total of 4 h to complete. For the determination of DOC concentration, duplicate 30 mL aliquots of this filtrate were kept in pre-combusted (450 °C, overnight) glass tubes, preserved with 36 µL 85% phosphoric acid (H_3PO_4) and sealed with a Teflon lined cap. Samples were stored at ambient temperature and in the dark until measurement. DOC concentration was measured on a Shimadzu total organic carbon (TOC) V_{CPH} analyzer following the method described in Rochelle-Newall et al. (2011). DOC concentration is expressed as mg of organic C per liter of water.

For CDOM (colored dissolved organic matter) measurements, 100-mL filtered samples were stored in pre-cleaned 125-mL amber glass bottles sealed with Teflon lined caps. After collection, the samples were stored frozen (− 20 °C) until measurement. Before the optical measurements, the samples were thawed slowly to room temperature and re-filtered at 0.2 µm (Sartorius Minisart NML Syringe filters). CDOM absorption was measured with a spectrophotometer (Analytica.Jena Specord 205 UV–VIS) from 200 to 750 nm using a 10 cm quartz cell and Milli-Q water as the blank.

Specific UV absorbance at 254 nm (SUVA) provides a proxy of DOM aromaticity (Weishaar et al. 2003) and was computed by dividing the UV absorbance at 254 nm by the concentration of DOC (mg C L^{-1}) (Hood et al. 2006). The spectral slope ratio, S_r was also calculated as the ratio of the slope of the shorter UV wavelength region (275–295 nm) to that of the longer UV wavelength region (350–400 nm) (Helms et al. 2008) and was obtained using linear regression on the log-transformed spectral ranges (Yamashita et al. 2010).

Excitation–emissions matrices (EEM) measurements were made on a Gilden Fluorosens fluorometer using a 1 cm quartz cuvette with 5 nm bandwidths for excitation and emission at an integration time of 100 ms. Excitation scans were made over a range of 200–450 nm at 5 nm increments and emission scans from 220 to 600 nm at 2.5 nm increment. EEMs were corrected for inner filter effects and the manufacturers' machine correction was applied. EEM fluorescence of Milli-Q water blank was subtracted from that of sample EEM, and EEM converted to Raman units (RU).

Humification (HIX) was calculated from excitation 255 nm as the ratio of the peak area under each curve at emission 434–480 nm and 300–346 nm. HIX indicates the humic content of DOM and ranges from 0 to 1 (Ohno 2002). The fluorescence index (FI) was measured as the ratio of fluorescence emission intensities at wavelength region of 470:520 nm and an excitation wavelength of 370 nm. The values of FI of less than 1.4 suggest a dominant terrestrial, higher-plant DOC source and the values of more than 1.4 suggest a predominant microbial DOC source (Cory et al. 2010).

PARAFAC analysis was carried out in MATLAB (version R2016a 9.0.0) with the DOMFluor toolbox for MATLAB (Murphy et al. 2013) to decompose the fluorescence signal into a series of tri-linear structures. Data processing was done to minimize the impact of scatter lines (removal of Rayleigh and Raman scatter). EEM wavelength ranges were reduced to excitation 290–450 nm and emission 300–600 nm. PARAFAC model generated three components using EEMs from our samples ($n = 16$). The three-component model (C1–C3) was validated using split-half and random initialization methods (Supp. Mats Figs. S1, S2).

Total suspended sediment (TSS) samples were grounded with an agate mortar, weighed and packed into tin containers (5 × 9 mm). Particulate organic carbon (POC) and total nitrogen (TN) concentrations, and stable C and N isotopes ($\delta^{13}C$ and $\delta^{15}N$) were measured using the Elementar® VarioPyro cube analyzer on line with a Micromass® Isoprime isotope ratio mass spectrometer (IRMS) facility (iEES-Paris, France) following the procedure described in Huon et al. (2017).

Assessment of bacterial diversity

DNA extraction and 16S rRNA gene sequencing

Fifty milliliters of each sample was first filtered through a 3 µm pore size filter (Polycarbonate Whatman) and a 0.2 µm (Polycarbonate Supor) filters to separate the particle-attached (PA) (> 3.0 µm) from free-living (FL) fractions

(< 3.0 µm and > 0.2 µm) (Crump et al. 1999). All filters were stored at − 20 °C until DNA extraction following a modified protocol adapted from Fuhrman et al. (1988). Briefly, the filters were cut in half using ethanol cleaned scissors and placed in separate Eppendorf® tubes. One tube was placed on ice and 525 µL of lysis buffer was added to start breaking Gram negative bacterial cells. The other tube was stored at − 20 °C as a back-up filter. Three cycles of freeze–thaw switches (65 °C for 2 min—ice for 5 min) were then performed to facilitate cell membrane breakage. Then 0.5 g of glass beads (Ø = 0.5 mm) was added into the tubes. The tubes were shaken for 45 s at 6 m s^{-1} using a Fastprep® (Millipore, Fastprep®-24, USA) and were incubated at 4 °C for 5 min; these steps were performed twice. Eleven microliters of lysozyme (1 mg mL^{-1}, final concentration) was added to the tube and left for 30 min at 37 °C to break down bacterial cell walls. Sodium dodecyl sulfate (SDS 10%) and proteinase K (final concentration, 100 µg mL^{-1}) were added to the tubes and were incubated at 55 °C for 2 h under constant shaking conditions (180 rpm) to remove the lipid membrane. A sodium chloride (NaCl 5 M) and a cetyltrimethylammonium bromide (CTAB) solution (final concentration, 1% in a 0.7 M NaCl solution) was added to the tubes, mixed and incubated at 65 °C for 10 min to separate DNA from protein. Nucleic acids were then extracted twice from digestion products with phenol–chloroform–isoamyl alcohol (25:24:1); the aqueous phase containing nucleic acids was kept and purified by adding phenol–chloroform–isoamyl alcohol (25:24:1). After isopropanol (0.6 volume) addition, the nucleic acids were precipitated at − 20 °C for 12 h. After centrifugation, the DNA pellet was rinsed with 99% pure ethanol to remove the salt previously added. The samples were spun 20 min at maximum speed (15,000 rpm) at 4 °C and the supernatants were removed. The DNA pellets were dried in a Speed Vac® (Labconco, USA) for 10 min and re-suspended in 50 µL of molecular cleaned distilled water. Nucleic acid extracts were stored at − 20 °C and sent overnight to Molecular Research Laboratories (Texas, USA) for further PCR amplification, product cleaning, library construction and high throughput sequencing.

The PCR primers 515F AGRGTTTGATCMTGGCTC AG and 806R GTNTTACNGCGGCKGCTG (Capone et al. 2011) with sample-specific barcodes on the forward primer were used to amplify the V4 variable region of the 16S rRNA gene. Thirty (30) cycles of PCR were performed using the HotStarTaq Plus Master Mix Kit (Qiagen, USA) under the following conditions: 94 °C for 3 min, followed by 28 cycles of 94 °C for 30 s, 53 °C for 40 s and 72 °C for 1 min, after which a final elongation step at 72 °C for 5 min was performed. After amplification, PCR products were checked in 2% agarose gel to determine the success of amplification, the relative intensity of bands and to check the expected amplicon size (291 bp). The samples included in this study were pooled together in equal proportions based on their molecular weight and DNA concentrations. Pooled PCR products were purified using calibrated Agencourt AMPure XP magnetic beads according to the manufacturer's instructions. The purified PCR product was then used to prepare a DNA library by following Illumina TruSeq DNA library preparation protocol. Sequencing was performed at MR DNA (http://www.mrdnalab.com, Shallowater, TX, USA) on an Illumina MiSeq machine following the manufacturer's guidelines.

Sequences processing and data analysis

The MOTHUR software (v. 1.33) was used to process 16S rRNA gene sequence reads following the standard operative protocol (Schloss et al. 2009). Short reads (< 250 bp) and reads with ambiguous primer or barcode sequences were discarded. Corresponding reads were paired in single sequences. Sequencing errors were reduced by aligning remaining reads to the SILVA database (Pruesse et al. 2007), screening the alignment to the overlapping region, and pre-clustering sequences distant by < 2 bp. Chimeric sequences were identified using the integrated version of UChime (Edgar et al. 2011) and removed accordingly. To avoid misinterpretation, sequences that were classified as "Chloroplast", "Mitochondria", or "unknown" lineages were removed before clustering into operational taxonomic units (OTUs). Rarefaction curves were calculated for all samples using the MOTHUR software (v.1.33). All samples were subsampled to 10,000 sequences before clustering into OTUs with a pairwise distance < 0.03 substitutions per nucleotide with the average neighbor method and considered for further analyses. Taxonomic assignments were performed on the alignment of consensus sequences with the RDP database (Cole et al. 2005). OTUs are classified to the finest taxonomic level possible from phylum to genus.

Alpha and Beta diversity assessment

Nonmetric multidimensional scaling (NMDS) based on Bray–Curtis dissimilarity were calculated to estimate the dissimilarity in structure between all samples using the metaMDS commands from the vegan package in R (Oksanen et al. 2017).

The ratio of shared OTUs between overland flow and stream water and the total number of OTUs in stream (FL-OTU and PA-OTU, for the FL and PA fractions, respectively) was determined for each fraction using:

$$\text{FL - OTU(or PA - OTU)} = \text{Shared OTU}_{\text{overland}} \div \text{Total OTU}_{\text{stream}},$$

where Shared $OTU_{overland}$ presents the number of shared OTU in the FL (or PA) fraction between Overland and Intermediate (or Downstream) and Total OTU_{stream} is the total number of OTU in the FL (or PA) fraction. Values close to

1 indicate a dominance of shared OTU (i.e. the samples are more similar) and values closer to 0 indicate a low proportion of shared OUT (i.e. the samples are more dissimilar).

A canonical correspondence analysis (CCA) was performed to determine the relationship between the significant environmental variables (DOC, S_r, SUVA254, fluorescence components (C1, C2 and C3) and TSS) and the stream PA or FL bacterial community fractions. Only OTUs with the total number of sequences > 10 was included in CCA.

The links between environmental factors (DOC concentration, fluorescence components, TSS) and bacterial OTUs were analyzed using network analysis for PA and FL separately. A correlation matrix was constructed by calculating all possible pairwise Spearman's rank correlations. Only OTUs with total number of sequences > 10 and an occurrence at least at 5 time points of the flood were taken into consideration. Results with a Spearman's correlation coefficient of $R > 0.7$ and a significance level of $p < 0.05$ were used to build the networks. Only positive correlations are shown in the networks. The nodes in each network represent OTUs or environmental factors and the edges that connect these OTUs show the correlation coefficients between OTUs. Node size corresponds to the number of sequences for each OTU. Networks were visualized in Gephi v. 0.9.1 using the Fruchterman–Reingold layout algorithm (Bastian et al. 2009).

Microbial putative functions were identified using FAPROTAX (functional annotation of prokaryotic taxa). The FAPROTAX software contains a database that converts taxonomic microbial community profiles into putative functional profiles, based on taxa identified in a sample (Louca et al. 2016). FAPROTAX was ran on the OTUs from the PA and FL fractions separately.

Statistical analyses

Correlations between environmental factors were estimated using the Pearson correlation coefficient with the Hmisc package in R (Harrell 2018). A one-way ANOSIM test was performed with Bray–Curtis dissimilarity using vegan packages in R to determine the significance of the difference in bacterial community structure. The betadisper function in vegan was used to test for homogeneity of variance between microbial communities in different sites for PA and FL separately to ensure the meeting of assumptions of the ANOSIM. The env.fit function was applied to the Bray–Curtis dissimilarity matrices (vegan package in R) (Oksanen et al. 2017) to evaluate the significance of relationship between PA and FL bacterial structure and the environment factors (DOC and CDOM). Differences were considered significant when the p value of the tests was lower than 0.05.

Results

Overland flow discharge during the 16 June 2014 storm flow event

At the Intermediate station, the maximum rainfall intensity occurred between 13:34 and 13:35 and reached 60 mm h^{-1}. The peak of flood occurred at 14:18 with a discharge of 33 L s^{-1} corresponding to 21% overland flow contribution using EC-based hydrograph separation. Overland flow peaked at 9 L s^{-1} between 14:33 and 14:35 (Fig. 2). At the Downstream station, rainfall peaked at 13:42 with an intensity of 156 mm h^{-1}. The peak of discharge (543 L s^{-1}) and overland flow (60% of total discharge) occurred at 14:00 (Fig. 3).

Environmental variables

The concentration of TSS at the Intermediate station increased during the flood rising stage from 17.5 mg L^{-1} prior to the flood to 1174.7 mg L^{-1} at flood peak and then decreased to 191.9 mg L^{-1} during the recession stage (Fig. 2). At the Downstream station, the TSS load reached a peak of 2195 mg L^{-1} following the peak of discharge and then declined to 409.3 mg L^{-1} at the end of flood event.

The temporal evolution of POC, C/N, $\delta^{13}C$ and $\delta^{15}N$ in TSS varied less at the Intermediate station than at the Downstream station over the course of the flood. The mean value of the C/N at the Downstream station was higher (11.8 ± 1.68) than at the Intermediate station (9.2 ± 0.4). Similarly, at the Downstream station, the mean values of $\delta^{13}C$ and $\delta^{15}N$ in TSS (-22.3 ± 0.8 and 7.2 ± 0.15, respectively) were higher than at the Intermediate station (-25.4 ± 0.34 and 6.5 ± 0.15, respectively) (Figs. 2, 3).

DOC results

DOC concentration at the Intermediate station increased during the rising stage of the flood. It increased from 2.6 mg L^{-1}, and peaked at 6.2 mg L^{-1} at 15:10 after the peak of flood it then decreased to 4.2 mg L^{-1} toward the end of the flood. Similarly, fluorescence index (FI), which indicates the ratio between allochthonous and autochthonous DOC contributions, gradually decreased during the rising flood. The index thereafter increased as the overland flow decreased. Humification (HIX) also gradually rose from 0.18 to 0.54 mg L^{-1}, meanwhile the aromaticity of DOC (SUVA) had a decreasing trend at the time of high allochthonous DOC supply. The inverse of molecular weight of DOC (S_r) remained relatively stable from 0.91 to

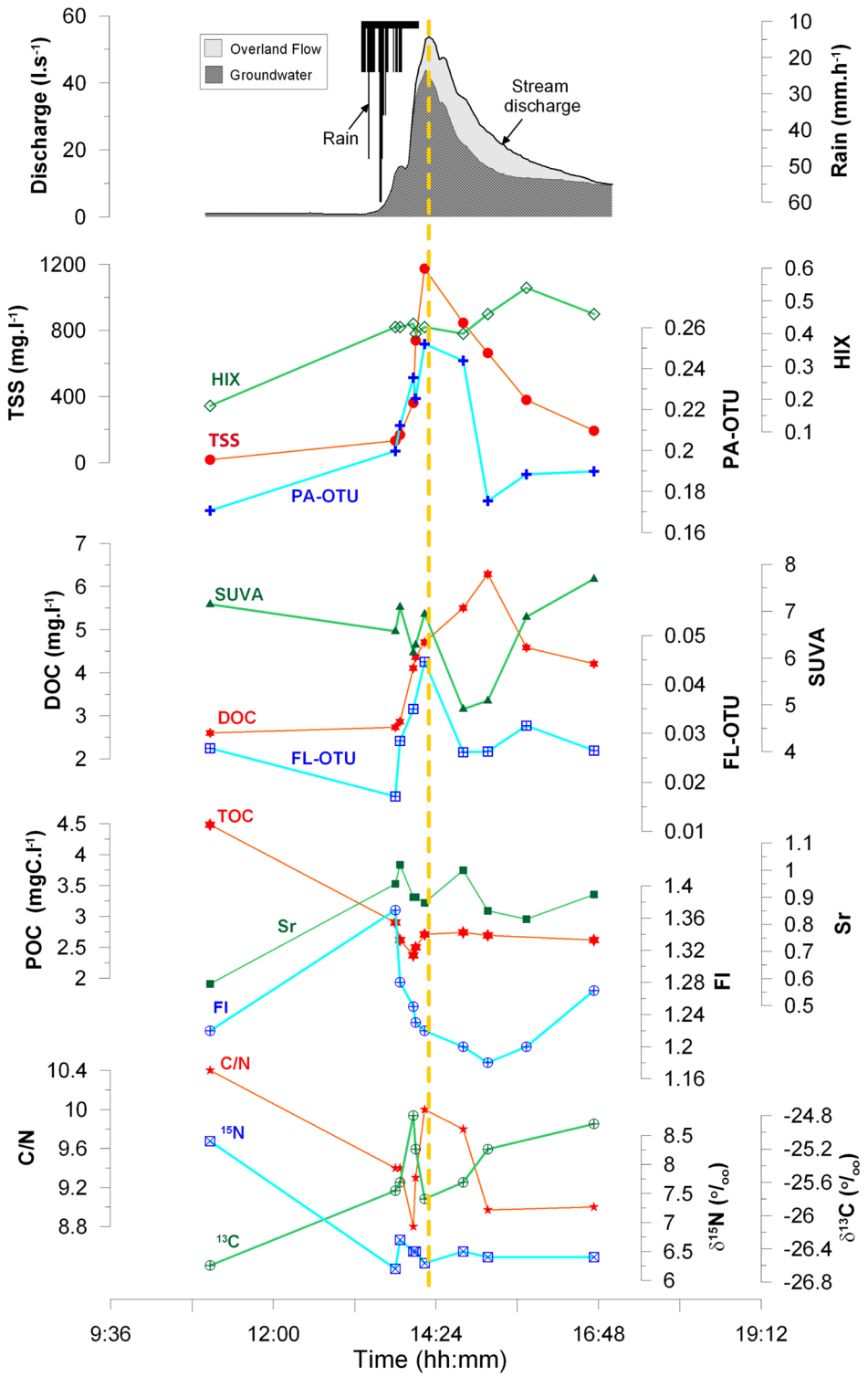

Fig. 2 Hydrograph (rain intensity and total discharge of ground water) and environmental variables measured during the flood event at the Intermediate station. Total suspended solid (TSS) concentration, particulate organic carbon (POC), stable C and N isotopes ($d^{13}C$ and $d^{15}N$) in TSS, particulate C/N ratio (C/N), dissolved organic carbon (DOC), fluorescence index (FI), the aromaticity of DOC (SUVA), humification (HIX), the inverse of molecular weight (S_r), PA-OTU and FL-OTU, the ratio of shared OTU number with overland flow (OF) in the stream water for particle attached (PA) and for free-living (FL). Each dot indicates a sampling event during the continuous measurements of discharge at the Intermediate station

1.02 during the flood event. The molecular weight of DOC was lower during the flood compared to base flow (Fig. 2).

At the Downstream station, DOC concentrations and HIX concomitantly peaked at 4.4 and 0.39 mg L^{-1}, respectively. Low FI (1.12) values also suggested the presence of more allochthonous DOC. The SUVA fluctuated from 4.97 to 6.18, but tended to rise with increasing DOC and discharge flow (Fig. 3) whereas S_r varied from 0.85 to 1.05, similar to the values recorded for the Intermediate station (Fig. 2).

During the progress of flood, DOC concentration, the aromaticity of DOC (SUVA) and humification (HIX) at the Intermediate station were higher than that at the

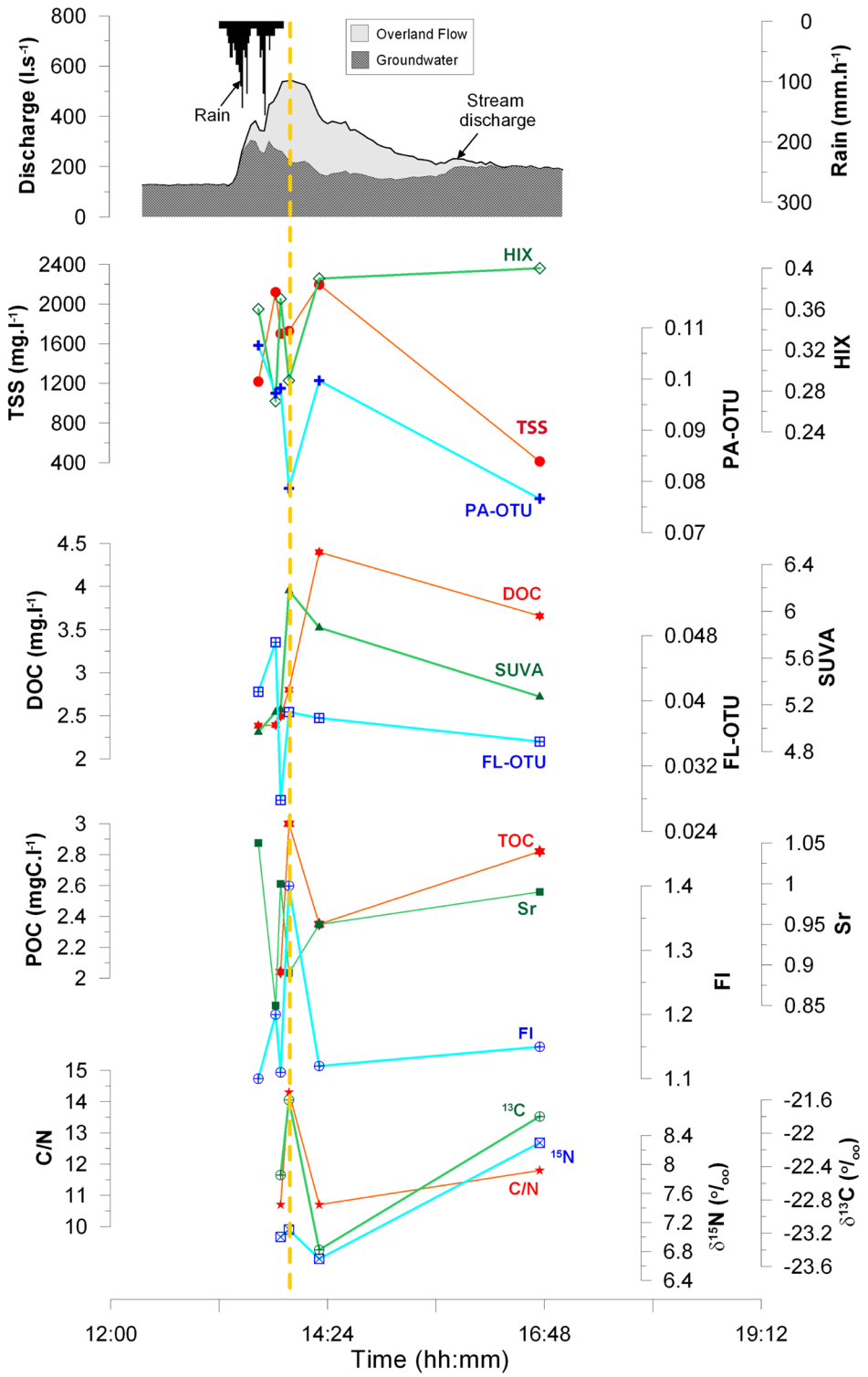

Fig. 3 Hydrograph (rain intensity and total discharge of ground water) and environmental variables measured during the flood event at the Downstream station. Total suspended solid (TSS) concentration, particulate organic carbon (POC), stable C and N isotopes ($d^{13}C$ and $d^{15}N$) in TSS, particulate C/N ratio (C/N), dissolved organic carbon (DOC), fluorescence index (FI), the aromaticity of DOC (SUVA), humification (HIX), the inverse of molecular weight (S_r), PA-OTU and FL-OTU, the ratio of shared OTU number with overland flow (OF) in the stream water for particle attached (PA) and for free-living (FL). Each dot indicates a sampling event during the continuous measurements of discharge at the Downstream station

Downstream station, in contrast to what was observed for TSS. Using the PARAFAC model, three components were identified as indicative components of optical characteristics of DOC (Table S1). Component 1 (C1) had a peak at excitation/emission (Ex/Em) wavelength of 340/457 corresponding to the UVC humic-like (peak C) (Fellman et al. 2010). Component 2 showed a peak of 420/475 for Ex/Em wavelength that is similar to the humic acid fraction (Yamashita et al. 2011). Component 3 had an Ex/Em peak of 300/352 similar to that previously identified as being tryptophan-like (Coble 1996; Yamashita and Tanoue 2003).

Bacterial community during the flood event

The number of observed OTUs (S_{obs}) and the estimated Chao richness of the PA bacterial community was significantly ($p < 0.05$) higher than for the FL bacterial community in stream during the flood event at both the Intermediate and Downstream stations (Table S2). The InvSimpson and Shannon index for both PA and FL had an increasing trend at the beginning of the flood and decreased at the end of flood at the Intermediate station (Table S2).

Shared OTUs between overland flow and stream water

The ratio between the number of shared OTUs between overland flow and stream water per total number of OTUs in stream indicates the contribution of bacterial community from overland flow to stream water during the flood event (Figs. 2, 3). At the Intermediate station, this ratio increased with discharge flow and overland flow at the beginning of the flood recession, from 0.17 to 0.25 for PA and from 0.01 to 0.04 for FL. The values then decreased at the end of the flood (Fig. 2). At the Downstream station, the ratio for the FL fraction varied slightly from 0.03 to 0.04 during the course of flood. The value for the PA fraction tended to decrease at the beginning of the flood event, thereafter it peaked again (0.09) concomitantly with the peaks of DOC, TSS and HIX (Fig. 3). In addition, the ratio of shared OTUs with overland flow in the stream water was higher in the PA than the FL fraction in both the Intermediate and Downstream stations.

Effect of environmental factors on bacterial community structure

Community structure was significantly separated between sites and between PA and FL fractions during the flood (ANOSIM, $R = 0.5$, $p = 0.001$). The PA fraction at the Intermediate and Downstream stations was more similar to the Overland station than was the FL fraction (Fig. 4). The relationships between environmental factors and the stream bacterial community were tested in canonical correlation analyses (CCA) and Monte Carlo permutation tests (999 permutations) for the stream PA and FL bacterial community fractions separately (Fig. 5; Table S3). The cumulative percentage of variance of the relationship between the bacterial community and environmental factors indicated that the first and second canonical axis explained 27.6% and 21.8% of this variance, respectively, for the PA fraction and 17.2% and 16% of this variance, respectively, for the FL fraction (Fig. 5). DOC, the humic component (C1) and TSS load

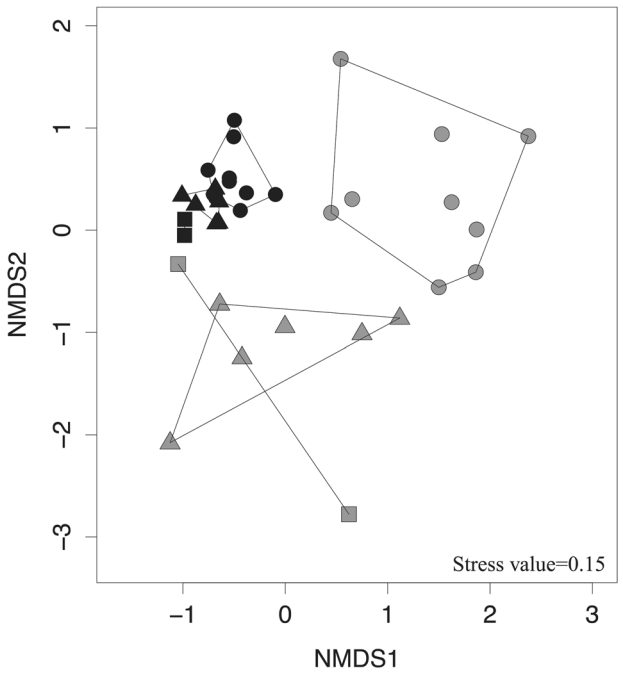

Fig. 4 Nonmetric multidimensional scaling (NMDS) based on Bray–Curtis distance for all samples in different sites for both particle attached (filled symbols) and free-living (open symbols) fractions during the flood at the hydrometric stations (Intermediate, Downstream and Overland stations). Circle: Intermediate station, triangle: Downstream station, square: Overland station. Note: due to low sequence cover, the sample 5 from the Intermediate station for free-living was removed

were significantly correlated with a shift in spatial bacterial structure between upstream and downstream for both PA and FL fractions (Fig. 5).

The relationship between environmental factors and bacterial community was assessed at the Intermediate station using network analysis (Fig. 6; Table S6). In the PA network, we found 9 OTUs belong to Proteobacteria (*Cupriavidus*, *Polyangiaceae*, *Rhizobiales*, *GR-WP33-30*, 2 OTUs of *SC-I-84*, 2 OTUs of *Phenylobacterium*, *Xanthomonadaceae*); 9 OTUs belong to Acidobacteria (8 OTUs of *Acidobacteriaceae* and *Candidatus_Koribacter*), 3 OTUs belong to Planctomycetes (2 OTUs of *Planctomycetaceae*, *Pirellula*), 2 OTUs belong to Firmicutes (*Anaerococcus*, *Epulopiscium*), 4 OTUs belong to Actinobacteria (*AKIW543*, *Propionibacterineae*) and 3 OTUs belong to other phylum (*Nitrospira*, *Chloroflexales*, *Opitutus).* The FL network has 6 OTUs belonging to Proteobacteria (*Rhodobium*, 2 OTUs of unclassified, *Pedomicrobium*, *Acinetobacter*, *Comamonadaceae*), 3 OTUs belong to Acidobacteria (*Acidobacteriaceae*), 1 OTUs belong to Planctomycetes (*Plantomycetaceae*), 1 OTU belong to Actinobacteria (AKIW543), 3 OTUs belong to other phylum (*DA101*, *Bacteroides*, *Opitutus*). The resulting

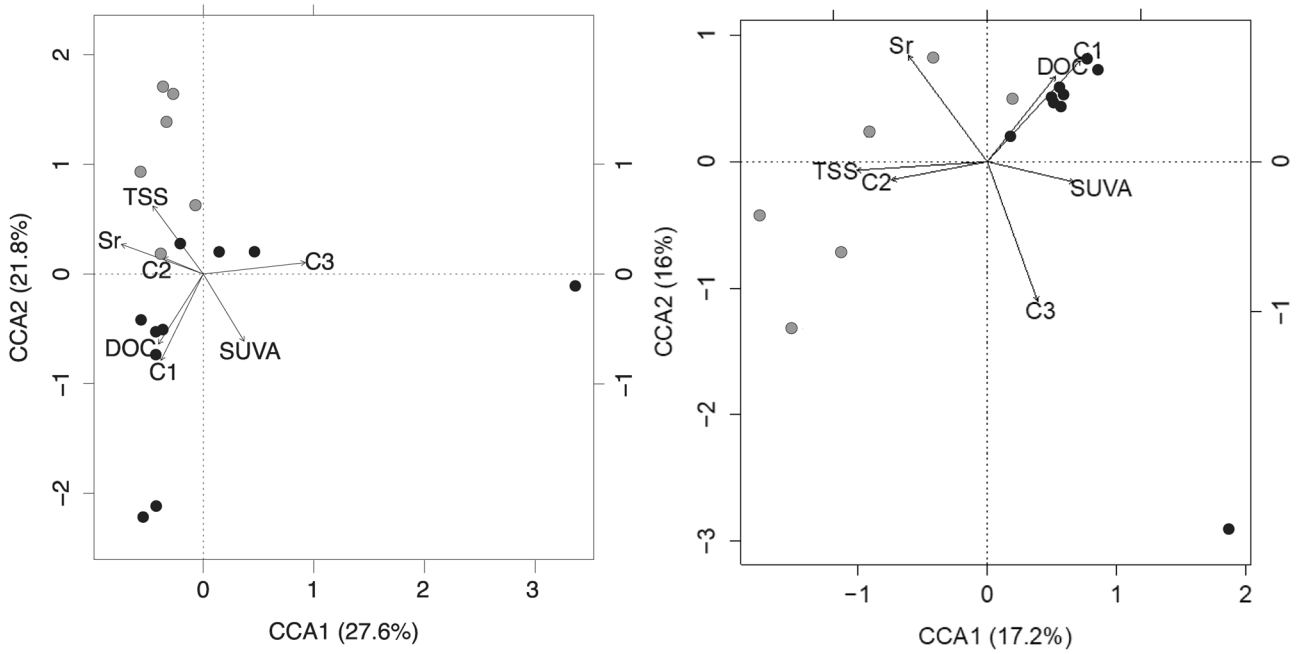

Fig. 5 Canonical correspondence analysis (CCA) analysis between environmental factors and bacterial community for the particles attached (left) and free-living fractions (right) for stream water sampled at the hydrometric stations the Intermediate (filled circle) and Downstream stations (open circle)

networks revealed that DOC was significantly associated with the humic components (C1 and C2) and TSS. These factors were significantly correlated with more PA-OTUs than FL-OTUs. For the PA fractions, DOC concentration was significantly correlated with 13 OTUs belonging to *Nitrospira*, *Propionibacterineae*, *Acidobacteriaceae*, *Xanthomonadaceae*, *Opitutus*, *Phenybacterium*, *AKIW543*, *Epulopiscium*, *Plantomycetaceae*, *Chloroflexales*. The genus of *Nitrospira* and *Acidobacteriaceae* were the most abundant OTUs amongst the OTUs related to DOC concentration. The humic component C2 was correlated with 6 OTUs including *Anaerococcus*, *Cupriavidus*, *Acidobacteriaceae*, *Plantomycetaceae*, *AKIW543*, *Chloroflexales.* TSS was correlated with 17 OTUs among which 5 OTUs were classified as *Acidobacteriaceae*, and the other as *SC-I-84* (3 OTUs), *Phenybacterium* 2 OTUs), *AKIW543* (2 OTUs), *Priellula* (1 OTUs), *Anaerococcus* (1 OTU), *Rhizobiales* (1 OTUs), *Candidatus_Koribacter* (1 OTU) and *GR-WP-33-30* (1 OTU).

For the FL fraction, DOC concentration was significantly correlated with 11 OTUs classified as *Acidobacteriaceae* (3 OTUs), *Pedomicrobium* (3 OTUs), *Bacteroides* (2 OTUs), *AKIW543* (1 OTU), *Opitutus* (1 OTU) and *Plantomycetaceae* (1 OTU). The humic component C2 was correlated with 3 OTUs including the genus *Rhodobium* and one OTU belonging to the *Gamma-Proteobacteria.* Meanwhile TSS was correlated with 3 OTUs including the genus of *Comanonadaceae*, *Pedomicrobium* and *Acidobacteriaceae*. The most abundant OTU in the network correlated with DOC concentration was from the *Acidobacteriaceae* (Fig. 6).

FAPROTAX assignations of the potential functional groups during the flood was possible for ~ 29.6% of the OTUs detected in PA samples and 20.4% of the OTUs detected in FL samples. The two most abundant functions in both fractions were chemoheterotrophy (from 25.4 to 36% for PA and from 20 to 39.4% for FL of total abundance of functional groups) and aerobic chemoheterotrophy (32.9% for PA and 31.2% for FL of total abundance of functional groups). Other abundant functional groups were aromatic compound degradation (0.2–5.8%), nitrate reduction (2–8.5%), fermentation (0.9–7%), nitrogen fixation (0.9–16.7%) and nitrate respiration (0.9–5%) for PA and fermentation (0.5–11.2%), nitrogen fixation (0.2–11.9%) and nitrate reduction (0.5–11.6%) for FL (Fig. S3a, b). Only nitrogen fixation was significantly different between the PA and FL fractions ($p < 0.003$).

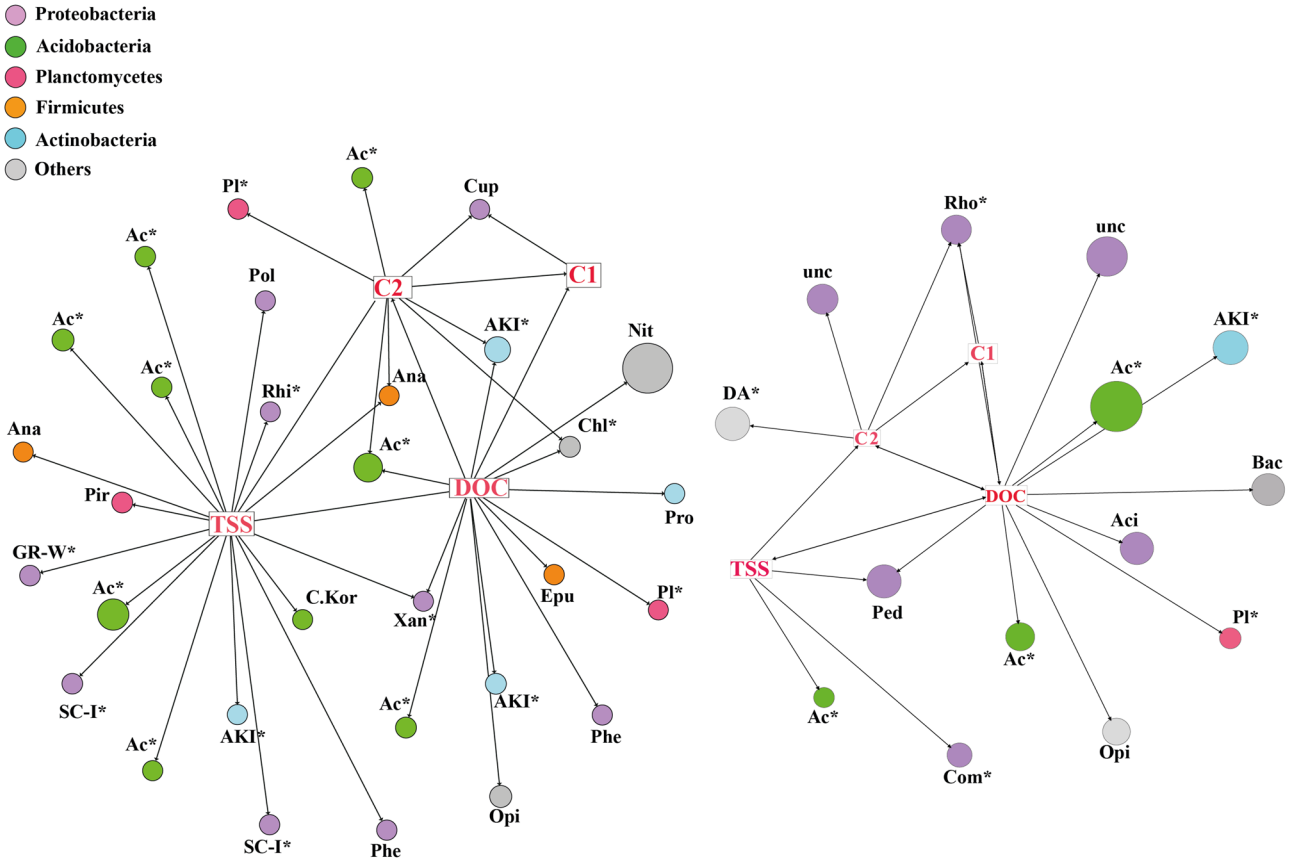

Fig. 6 Network analysis of relationship between environmental factors: dissolved organic carbon (DOC), humic components (Parafac) (C1, C2), total suspended sediment (TSS) and particle attached-OTUs (left panel) and free-living—OTUs (right panel). Node colors indicate the bacterial phylum, node labels indicate genus. Node size is proportional to the number of sequences. The OTUs are listed in Table S6. *Unidentified OTUs belonging to family or order level

Discussion

Source and composition of particle borne organic matter in TSS and DOC in stream water during the flood event

The peak of TSS was synchronous with discharge during the flood course at the Intermediate station but not at the Downstream station. This variability in synchronicity between flood and TSS peaks has already been shown for this system and is due to a variety of factors, such as rain height, spatial distribution and intensity (Boithias et al. 2021a). Huon et al. (2017) have previously observed that the evolutions of POC, POC/PN, $\delta^{13}C$ and $\delta^{15}N$ in TSS at the Intermediate station follow hyperbolic trends with suspended sediment loads, reflecting the dilution of particle borne organic matter by in-channel or allochthonous mineral matter supply. The low value of $\delta^{13}C$ (-25.4 ± 0.34) at the Intermediate station in our study matches the mean surface soil, reflecting the dominance of C3 photosynthesis pathway plants (upland rice, fallow vegetation and teak plantation) across the catchment (Huon et al. 2013, 2017; Gourdin et al. 2015). The $\delta^{13}C$, $\delta^{15}N$ in TSS values at the Downstream station were higher than in the upper parts of the catchment (the Intermediate station) and matched subsurface soil signatures (stream banks and gullies). This reflects both the input of C4-plant derived organic matter originating from swamps covered with Napier grass along the Houay Xon catchment and of subsurface particles supplied by channel banks and gullies (Huon et al. 2013, 2017; Gourdin et al. 2015). Our results are in accordance with these conclusions that surface soil is the dominant potential source of particles from cultivated areas in the upper catchment parts (Huon et al. 2017) and that sediment remobilization processes play a key role in downstream areas (Gourdin et al. 2014b).

DOC concentration did not concomitantly peak with discharge. However, DOC concentration increased during the rising stage, suggesting an increase in the inflow of soil derived DOC into the stream. Similar, significant increases in DOC have been observed in the Hunter river and its tributaries in Australia, after a major flood event (Carney et al. 2015) and Besemer et al. (2005) found that flood events

increased the amount of DOM, probably as a consequence of inputs from previously disconnected pools and increased terrestrial inflows. The decrease of FI, a proxy of DOC origin, with increasing DOC concentration during the flood course also points towards the allochthonous origin of DOC in overland flow (Fellman et al. 2010) as do the PARAFAC components (C1–C3) that considered to be characteristic of humic-like substances (Fellman et al. 2010; Yamashita et al. 2011). Finally, compared to before the flood event, a decrease of $SUVA_{254}$ and of molecular weight (increase of S_r) at high flow at the Intermediate station indicated that the composition of the DOC released during the flood event was less aromatic and of lower molecular weight. Fellman et al. (2008b) showed that a high SUVA is associated with lower bioavailability and biodegradation is known to increase the aromaticity of DOM (Kalbitz 2003). Therefore, the DOC at the Intermediate station during the flood event was probably less degraded, less aromatic and more bioavailable (Buffam et al. 2001; McLaughlin and Kaplan 2013). This suggests that soil water comprised more fresh, less degraded DOC than in stream water at base flow (Evans et al. 2007). In contrast to our results, some studies have reported that the aromatic content of DOM (SUVA) increased with storm discharge (Hood et al. 2006; Fellman et al. 2009; Inamdar et al. 2011). The explanation for this difference is not clear, but may be related to pedoclimatic characteristics, soil type and soil organic matter origin in the catchment. Our SUVA values are high compared to the range of published values and it is important to keep this caveat in mind. This difference may be related the factors mentioned above or to interference from Fe or other solutes (Weishaar et al. 2003). As we were unable to analyze the samples directly in the field, we had opted to freeze the samples and this may also explain the high values. Several articles have looked at the question of storage with sometimes contrasting results (Fellman et al. 2008a; Rochelle-Newall et al. 2014), it is therefore difficult at this stage to determine the reason for these high values.

Overland flow drives bacterial community structure during the flood event

We observed an increase in richness of bacteria during the flood as compared to base flow. This was driven by the dispersal of the PA bacteria originating from overland flow during the rising stage of the flood (Fig. 2) as indicated by the closeness between the structure of the stream water PA fraction to that from the Overland station as compared to the stream water FL fraction. Besemer et al. (2005) indicated, in a temperate river-floodplain system, that compared to the FL fraction the PA bacterial fraction was probably more strongly impacted by changes in hydrological and environmental conditions such as the inflow of terrestrial organic matter. Moreover, Adams et al. (2014) found, during large storm events, that the high dispersal rate periodically disrupts a stable community composition, resulting in a similar bacterial community between inlet and outlet. In our data, the similarity between PA fraction from Overland, Intermediate and Downstream also reflects this dispersion. Such strong impacts of super storms on freshwater bacterial community composition and function have also been previously observed elsewhere (Ulrich et al. 2016; Kan 2018).

The Overland station is located within a teak plantation. Previous work has underlined the strong negative impact of teak plantation on soil erosion (Ribolzi et al. 2017) and other work from this catchment has underlined the influence of past and present vicinal land cover on bacterial community structure and organic carbon in soils and in overland flow (Le et al. 2020). The similarity of PA fractions between the Overland, Intermediate and Downstream stations (Fig. 4) suggests that the source of the PA fraction was soils that were washed out from under teak plantations via overland flow during the flood event. The higher proportions of allochthonous DOC and OTUs' ratios exported from overland flow into stream water at the Intermediate station relative to the Downstream station point towards a stronger effect of overland flow at the Intermediate station. Moreover, although the stream received overland flow during the flood, this mixture of flow from the basin hillslopes and groundwater was rapidly washed out as a consequence of the high flood discharge rate. This mechanism probably explains why the ratio of OTUs from overland flow in the stream water decreases (i.e. is less similar) at the end of the flood.

Relationship between bacterial community structure and environmental variables

We found that TSS was one of the most important factors driving bacterial community composition for both PA and FL at different sites during the flood. Staley et al. (2015) observed that particle sediment bacterial community composition strongly influenced water column bacterial community structure. Luef et al. (2007) also proposed that the PA fraction was more affected by particle composition rather than by the hydrological characteristics of the system. Tang et al. (2017) also indicated that turbidity or TSS (an indicator of sediment and phytodetritus resuspension) was one of the main factors controlling the structure of bacterial communities in the PA fraction. Thus, storm water influx and the associated sediments in free-flowing water are probably the principal factor influencing bacterial community structure during the flood (Ulrich et al. 2016; Kan 2018).

In our study, the connection between particle composition sources rather than hydrological regime played a key role in driving the bacterial community. DOC and humic components were more related to the temporal shift in the PA bacterial community than in the FL fraction because the

PA community structure changed with increasing DOC concentration during the water level rising stage (Fig. 4). This pattern is supported by the network analysis, which shows that more PA-OTUs were significantly correlated with DOC, the humic components and TSS than FL-OTUs. Similarly, DOC and the humic components were found to have a more important role in PA co-occurrence networking than for the FL fraction in this catchment at base flow in the wet season (Le et al. 2018). This suggests that the stream bacterial community was driven by upland soil supply through hydrological connectivity at base flow (Le et al. 2018) and by overland flow during the flood event (this work).

The genus *Nitrospira*, the most abundant OTU in the PA fraction, was correlated to DOC concentration in stream water during the flood event. *Nitrospira* is an aerobic, nitrite-oxidizing bacterium and through its role in the nitrification process this bacterium plays a key role in soil N dynamics (Daims et al. 2015; Le Roux et al. 2016). *Nitrospira* has also been identified as possessing a substantial metabolic versatility in the utilization of organic compounds and urea degradation (Daims et al. 2015; Gruber-Dorninger et al. 2015; Koch et al. 2015). This suggests that the loss of this taxa and other taxa in overland flow into stream water may shift in-stream metabolic function.

FAPROTAX (Fig. S3) revealed that the two most abundant functions in both PA and FL were chemoheterotrophy and aerobic chemoheterotrophy. These functions were also found to be abundant in soil and runoff water during a rain simulation in the same catchment (Lamers et al. 2006). Almost all of the genera found correlated with DOC concentration, for example *Nitrospira*, *Propionibacterineae*, *Acidobacteriaceae*, *Xanthomonadaceae*, *Opitutus*, *Acidobacteriaceae* and all belong to the functional group aerobic chemoheterotrophy.

Moreover, the functional groups relating to the nitrogen cycle such as nitrogen fixation, nitrate respiration, and nitrate reduction were abundant in the different sites, especially in the PA community. This corresponds to the results from Le et al. (2018) in the same catchment who observed that the functional groups for nitrate reduction and respiration were more abundant in runoff from upland rice planted soils.

Conclusion

During the flood event, stream water was strongly influenced by overland flow and its associated characteristics including allochthonous DOC, POC and the particle-bound bacterial community. The number of PA taxa originating from overland flow increased in stream water as the flood progressed and was higher than that of FL taxa. This means that the PA fraction is more dependent on eroded particle material flow from hillslope terrestrial runoff than is the FL fraction. The higher representation of specific taxa (e.g. *Nitrospira*, *Acidobacteriaceae*) also points towards a strong impact of overland flow on aquatic microbial ecosystem function. This study provides fundamental insights into our understanding of how the transportation of the soil bacterial community, via overland flow, impacts the stream bacterial community during a flood event, underlining the biological connectivity between terrestrial runoff and stream flow.

Supplementary Information The online version contains supplementary material available at https://doi.org/10.1007/s00027-021-00839-y.

Acknowledgements The authors are grateful to the Lao PDR Department of Agricultural Land Management (DALaM). We also thank the M-TROPICS Critical Zone Observatory (https://mtropics.obs-mip.fr/), which belongs to the French Research Infrastructure OZCAR (http://www.ozcar-ri.org/), for the logistic support. Julie Legoupi is thanked for her help with the figures. This work forms part of the Ph.D. thesis requirements of HL who was financed by a Ph.D. grant from the USTH, Vietnam and the IRD (ARTS).

Funding This study was funded by the Institute of Research for sustainable Development (IRD, main funding), the French National Research Agency (TecItEasy project, ANR-13-AGRO-0007).

Data availability The data are published on the DataSuds site of the IRD as Le et al. (2021) at http://doi.org/10.23708/K95OKX.

Declarations

Conflict of interest The authors declare no conflict of interest or competing interest.

References

Adams HE, Crump BC, Kling GW (2014) Metacommunity dynamics of bacteria in an arctic lake: the impact of species sorting and mass effects on bacterial production and biogeography. Front Microbiol 5:82

Agren A, Berggren M, Laudon H, Jansson M (2008) Terrestrial export of highly bioavailable carbon from small boreal catchments in spring floods. Freshw Biol 53:964–972

Ali G, Roy A (2010) Shopping for hydrologically representative connectivity metrics in a humid temperate forested catchment. Water Resour Res. https://doi.org/10.1029/2010WR009442

Banach AM, Banach K, Visser EJW, Stępniewska Z, Smits AJM, Roelofs JGM, Lamers LPM (2009) Effects of summer flooding on floodplain biogeochemistry in Poland; implications for increased flooding frequency. Biogeochemistry 92:247–262

Bastian M, Heymann S, Jacomy M (2009) Gephi: an open source software for exploring and manipulating networks. Int Conf Web Soc Media 8:361–362

Belnap J, Welter JR, Grimm NB, Barger N, Ludwig JA (2005) Linkages between microbial and hydrologic processes in arid and semiarid watersheds. Ecology 82:298–307

Besemer K, Moeseneder MM, Arrieta JM, Herndl GJ, Peduzzi P (2005) Complexity of bacterial communities in a river-floodplain system (Danube, Austria). Appl Environ Microbiol 71:609–620

Boithias L, Ribolzi O, Lacombe G, Thammahacksa C, Silvera N, Latsachack K et al (2021a) Quantifying the effect of overland

flow on *Escherichia coli* pulses during floods: use of a tracer-based approach in an erosion-prone tropical catchment. J Hydrol 594:125935
Boithias L, Auda Y, Audry S, Bricquet J-P, Chanhphengxay A, Chaplot V et al (2021b) The multiscale TROPIcal CatchmentS critical zone observatory M-TROPICS dataset II: land use, hydrology and sediment production monitoring in Houay Pano, northern Lao PDR. Hydrol Process 35:e14126
Buffam I, Galloway JN, Blum LK, McGlathery KJ (2001) A stormflow/baseflow comparison of dissolved organic matter concentrations and bioavailability in an Appalachian stream. Biogeochemistry 53:269–306
Capone KA, Dowd SE, Stamatas GN, Nikolovski J (2011) Diversity of the human skin microbiome early in life. J Investig Dermatol 131:2026–2032
Carney RL, Mitrovic SM, Jeffries T, Westhorpe D, Curlevski N, Seymour JR (2015) River bacterioplankton community responses to a high inflow event. Aquat Microb Ecol 75:187–205
Carvalho P, Thomaz SM, Bini LM (2003) Effects of water level, abiotic and biotic factors on bacterioplankton abundance in lagoons of a tropical floodplain (Paraná River, Brazil). Hydrobiologia 510:67–74
Causse J, Billen G, Garnier J, Henri-des-Tureaux T, Olasa X, Thammahacksa C et al (2015) Field and modelling studies of *Escherichia coli* loads in tropical streams of montane agro-ecosystems. J Hydroenvironment Res 9:496–507
Chaplot VAM, Rumpel C, Valentin C (2005) Water erosion impact on soil and carbon redistributions within uplands of Mekong River. Glob Biogeochem Cycles. https://doi.org/10.1029/2005GB002493
Coble PG (1996) Characterization of marine and terrestrial DOM in seawater using excitation emission matrix spectroscopy. Mar Chem 51:325–346
Cole JR, Chai B, Farris RJ, Wang Q, Kulam SA, McGarrell DM et al (2005) The ribosomal database project (RDP-II): sequences and tools for high-throughput rRNA analysis. Nucleic Acids Res 33:D294–D296
Cory RM, Miller MP, McKnight DM, Guerard JJ, Miller PL (2010) Effect of instrument-specific response on the analysis of fulvic acid fluorescence spectra. Limnol Oceanogr Methods 8:67–78
Crump BC, Armbrust EV, Baross JA (1999) Phylogenetic analysis of particle-attached and free-living bacterial communities in the Columbia River, its estuary, and the adjacent coastal ocean. Appl Environ Microbiol 65:3192–3204
Daims H, Lebedeva EV, Pjevac P, Han P, Herbold C, Albertsen M et al (2015) Complete nitrification by *Nitrospira* bacteria. Nature 528:504–509
Eccles R, Zhang H, Hamilton D (2019) A review of the effects of climate change on riverine flooding in subtropical and tropical regions. J Water Clim Change 10:687–707
Edgar RC, Haas BJ, Clemente JC, Quince C, Knight R (2011) UCHIME improves sensitivity and speed of chimera detection. Bioinformatics 27:2194–2200
Evans C, Freeman C, Cork L, Thomas D, Reynolds B, Billett M et al (2007) Evidence against recent climate-induced destabilisation of soil carbon from 14C analysis of riverine dissolved organic matter. Geophys Res Lett 34:L07407
Evrard O, Laceby JP, Huon S, Lefèvre I, Sengtaheuanghoung O, Ribolzi O (2016) Combining multiple fallout radionuclides (137Cs, 7Be, 210Pbxs) to investigate temporal sediment source dynamics in tropical, ephemeral riverine systems. J Soils Sediments 16:1130–1144
Fellman JB, D'Amore DV, Hood E (2008a) An evaluation of freezing as a preservation technique for analyzing dissolved organic C, N and P in surface water samples. Sci Total Environ 392:305–312
Fellman JB, D'Amore DV, Hood E, Boone RD (2008b) Fluorescence characteristics and biodegradability of dissolved organic matter in forest and wetland soils from coastal temperate watersheds in southeast Alaska. Biogeochemistry 88:169–184
Fellman JB, Hood E, Edwards RT, D'Amore DV (2009) Changes in the concentration, biodegradability, and fluorescent properties of dissolved organic matter during stormflows in coastal temperate watersheds. J Geophys Res. https://doi.org/10.1029/2008JG000790
Fellman JB, Hood E, Spencer RGM (2010) Fluorescence spectroscopy opens new windows into dissolved organic matter dynamics in freshwater ecosystems: a review. Limnol Oceanogr 55:2452–2462
Fuhrman JA, Comeau DE, Hagstrom A, Chan AM (1988) Extraction from natural planktonic microorganisms of DNA suitable for molecular biological studies. Appl Environ Microbiol 54:1426–1429
Gourdin E, Evrard O, Huon S, Lefèvre I, Ribolzi O, Reyss J-L et al (2014a) Suspended sediment dynamics in a Southeast Asian mountainous catchment: combining river monitoring and fallout radionuclide tracers. J Hydrol 519:1811–1823
Gourdin E, Evrard O, Huon S, Reyss JL, Ribolzi O, Bariac T et al (2014b) Spatial and temporal variability of Be-7 and Pb-210 wet deposition during four successive monsoon storms in a catchment of northern Laos. J Environ Radioact 136:195–205
Gourdin E, Huon S, Evrard O, Ribolzi O, Bariac T, Sengtaheuanghoung O, Ayrault S (2015) Sources and export of particle-borne organic matter during a monsoon flood in a catchment of northern Laos. Biogeosciences 12:1073–1089
Gruber-Dorninger C, Pester M, Kitzinger K, Savio DF, Loy A, Rattei T et al (2015) Functionally relevant diversity of closely related Nitrospira in activated sludge. ISME 9:643–655
Harrell FEJ (2018) Hmisc: Harrell miscellaneous. R package version 4.1-1. http://CRAN.R-project.org/package=Hmisc. Accessed 15 Nov 2019
Helms JR, Stubbins A, Ritchie JD, Minor EC, Kieber DJ, Mopper K (2008) Absorption spectral slopes and slope ratios as indicators of molecular weight, source, and photobleaching of chromophoric dissolved organic matter. Limnol Oceanogr 53:955–969
Hood E, Gooseff MN, Johnson SL (2006) Changes in the character of stream water dissolved organic carbon during flushing in three small watersheds. Or J Geophys Res 111:G01007
Huon S, De Rouw A, Bonte P, Robain H, Valentin C, Lefevre I et al (2013) Long-term soil carbon loss and accumulation in a catchment following the conversion of forest to arable land in northern Laos. Agric Ecosyst Environ 169:43–57
Huon S, Evrard O, Gourdin E, Lefèvre I, Bariac T, Reyss J-L et al (2017) Suspended sediment source and propagation during monsoon events across nested sub-catchments with contrasted land uses in Laos. J Hydrol Reg Stud 9:69–84
Inamdar S, Singh S, Dutta S, Levia D, Mitchell M, Scott D et al (2011) Fluorescence characteristics and sources of dissolved organic matter for stream water during storm events in a forested mid-Atlantic watershed. J Geophys Res. https://doi.org/10.1029/2011jg001735
Kalbitz K (2003) Changes in properties of soil-derived dissolved organic matter induced by biodegradation. Soil Biol Biochem 35:1129–1142
Kan J (2018) Storm events restructured bacterial community and their biogeochemical potentials. J Geophys Res Biogeosci 123:2257–2269
Kirchman DL, Dittel AI, Findlay SEG, Fischer D (2004) Changes in bacterial activity and community structure in response to dissolved organic matter in the Hudson River, New York. Aquat Microb Ecol 35:243–257
Koch H, Lücker S, Albertsen M, Kitzinger K, Herbold C, Spieck E et al (2015) Expanded metabolic versatility of ubiquitous nitrite-oxidizing bacteria from the genus Nitrospira. Proc Natl Acad Sci USA 112:11371–11376

Lamers L, Loeb R, Antheunisse A, Miletto M, Lucassen E, Boxman A et al (2006) Biogeochemical constraints on the ecological rehabilitation of wetland vegetation in river floodplains. Hydrobiologia 565:165–186

Le Roux X, Bouskill NJ, Niboyet A, Barthes L, Dijkstra P, Field CB et al (2016) Predicting the responses of soil nitrite-oxidizers to multi-factorial global change: a trait-based approach. Front Microbiol 7:628

Le HT, Rochelle-Newall E, Yves Auda OR, Sengtaheuanghoung O, Thébault E, Soulileuth B, Pommier T (2018) Vicinal land use change strongly drives stream bacterial community in a tropical montane catchment. FEMS Microbiol Ecol 94:1–15

Le HT, Rochelle-Newall E, Ribolzi O, Janeau JL, Huon S, Latsachack K, Pommier T (2020) Land use strongly influences soil organic carbon and bacterial community export in runoff in tropical uplands. Land Degrad Dev 31:118–132

Le TH, Pommier T, Ribolzi O, Soulileuth B, Huon S, Silvera N, Rochelle-Newall E (2021) Dataset of flood event in Houay Pano catchment, Laos on June 16th, 2014. DataSuds. https://doi.org/10.23708/K95OKX

Lindström ES, Langenheder S (2012) Local and regional factors influencing bacterial community assembly. Environ Microbiol Rep 4:1–9

Louca S, Jacques SMS, Pires APF, Leal JS, Srivastava DS, Parfrey LW et al (2016) High taxonomic variability despite stable functional structure across microbial communities. Nat Ecol Evol. https://doi.org/10.1038/s41559-016-0015

Luef B, Aspetsberger F, Hein T, Huber F, Peduzzi P (2007) Impact of hydrology on free-living and particle-associated microorganisms in a river floodplain system (Danube, Austria). Freshw Biol 52:1043–1057

Maiga-Yaleu S, Guiguemde I, Yacouba H, Karambiri H, Ribolzi O, Bary A et al (2013) Soil crusting impact on soil organic carbon losses by water erosion. CATENA 107:26–34

Marengo JA, Espinoza JC (2016) Extreme seasonal droughts and floods in Amazonia: causes, trends and impacts. Int J Climatol 36:1033–1050

McLaughlin C, Kaplan LA (2013) Biological lability of dissolved organic carbon in stream water and contributing terrestrial sources. Freshw Sci 32:1219–1230

Mügler C, Ribolzi O, Viguier M, Janeau J-L, Jardé E, Latsachack K et al (2021) Experimental and modelling evidence of splash effects on manure borne Escherichia coli washoff. Environ Sci Pollut Res. https://doi.org/10.1007/s11356-021-13011-8

Murphy KR, Stedmon CA, Graeber D, Bro R (2013) Fluorescence spectroscopy and multi-way techniques. PARAFAC Anal Methods 5:6557–6566

Nakhle P, Ribolzi O, Boithias L, Rattanavong S, Auda Y, Sayavong S et al (2021) Effects of hydrological regime and land use on in-stream *Escherichia coli* concentration in the Mekong basin, Lao PDR. Sci Rep 11:3460

Ohno T (2002) Fluorescence inner-filtering correction for determining the humification index of dissolved organic matter. Environ Sci Technol 36:742–746

Oksanen J, Blanchet GF, Friendly M, Kindt R, Legendre P, McGlinn D et al (2017) Vegan: community ecology package. R package version 2.4-5. http://CRAN.R-project.org/package=vegan. Accessed 6 Jan 2018

Patin J, Mouche E, Ribolzi O, Sengtahevanghoung O, Latsachak KO, Soulileuth B et al (2018) Effect of land use on interrill erosion in a montane catchment of Northern Laos: an analysis based on a pluri-annual runoff and soil loss database. J Hydrol 563:480–494

Poeppl R, Keiler M, Von Elverfeldt K, Zweimueller I, Glade T (2012) The influence of riparian vegetation cover on diffuse lateral sediment connectivity and biogeomorphic processes in a medium-sized agricultural catchment, Austria. Geogr Ann Ser A Phys Geogr 94:511–529

Polade SD, Gershunov A, Cayan DR, Dettinger MD, Pierce DW (2017) Precipitation in a warming world: assessing projected hydro-climate changes in California and other Mediterranean climate regions. Sci Rep. https://doi.org/10.1038/s41598-017-11285-y

Pruesse E, Quast C, Knittel FB, Ludwig W, Peplies J, Glöckner FO (2007) SILVA: a comprehensive online resource for quality checked and aligned ribosomal RNA sequence data compatible with ARB. Nucleic Acids Res 35:7188–7196

Ribolzi O, Moussa R, Gaudu JC, Valles V, Voltz M (1997) Stream water regime change at autumn recharge on a Mediterranean farmed catchment using a natural tracer. C R L'academie Sci 324:985–992

Ribolzi O, Evrard O, Huon S, Rochelle-Newall E, Henri-des-Tureaux T, Silvera N et al (2016) Use of fallout radionuclides ((7)Be, (210)Pb) to estimate resuspension of Escherichia coli from streambed sediments during floods in a tropical montane catchment. Environ Sci Pollut Res 23:3427–3435

Ribolzi O, Evrard O, Huon S, de Rouw A, Silvera N, Latsachack KO et al (2017) From shifting cultivation to teak plantation: effect on overland flow and sediment yield in a montane tropical catchment. Sci Rep 7:1–12

Ribolzi O, Lacombe G, Pierret A, Robain H, Sounyafong P, de Rouw A, Soulileuth B, Mouche E, Huon S, Silvera N, Latxachak KO, Sengtaheuanghoung O, Valentin C (2018) Interacting land use and soil surface dynamics control groundwater outflow in a montane catchment of the lower Mekong basin. Agric Ecosyst Environ 268:90–102

Richter M (2016) Classifications of climates in the tropics. In: Pancel L, Köhl M (eds) Tropical forestry handbook. Springer, Berlin, Heidelberg. https://doi.org/10.1007/978-3-642-54601-3_35

Rochelle-Newall EJ, Chu VT, Pringault O, Amouroux D, Arfi R, Bettarel Y et al (2011) Phytoplankton diversity and productivity in a highly turbid, tropical coastal system (Bach Dang Estuary, Vietnam). Mar Pollut Bull 62:2317–2329

Rochelle-Newall E, Hulot FD, Janeau JL, Merroune A (2014) CDOM fluorescence as a proxy of DOC concentration in natural waters: a comparison of four contrasting tropical systems. Environ Monit Assess 186:589–596

Schloss PD, Westcott SL, Ryabin T, Hall JR, Hartmann M, Hollister EB et al (2009) Introducing mothur: open source, platform-independent, community-supported software for describing and comparing microbial communities. Appl Environ Microbiol 75:7537–7541

Staley C, Gould TJ, Wang P, Phillips J, Cotner JB, Sadowsky MJ (2015) Species sorting and seasonal dynamics primarily shape bacterial communities in the Upper Mississippi River. Sci Total Environ 505:435–445

Syed KH, Goodrich DC, Myers DE, Sorooshian S (2003) Spatial characteristics of thunderstorm rainfall fields and their relation to runoff. J Hydrol 217:1–21

Talbot CJ, Bennett EM, Cassell K et al (2018) The impact of flooding on aquatic ecosystem services. Biogeochemistry 141:439–461

Tang X, Chao J, Gong Y, Wang Y, Wilhelm SW, Gao G (2017) Spatiotemporal dynamics of bacterial community composition in large shallow eutrophic Lake Taihu: high overlap between free-living and particle-attached assemblages. Limnol Oceanogr 62:1366–1382

Trenberth KE (2011) Changes in precipitation with climate change. Clim Res 47:123–138

Trevisani S, Cavalli M (2016) Topography-based flow-directional roughness: potential and challenges. Earth Surf Dyn 4:343–358

Ulrich N, Rosenberger A, Brislawn C, Wright J, Kessler C, Toole D et al (2016) Restructuring of the aquatic bacterial community by

hydric dynamics associated with superstorm sandy. Appl Environ Microbiol 82:3525–3536
Valentin C, Bresson LM (1992) Morphology, genesis and classification of surface crusts in loamy and sandy soils. Geoderma 55:225–245
Weishaar JL, Aiken GR, Bergamaschi BA, Fram MS, Fujii R, Mopper K (2003) Evaluation of specific ultraviolet absorbance as an indicator of the chemical composition and reactivity of dissolved organic carbon. Environ Sci Technol 37:4702–4708
Yamashita Y, Tanoue E (2003) Chemical characterization of protein-like fluorophores in DOM in relation to aromatic amino acids. Mar Chem 82:255–271
Yamashita Y, Maie N, Briceno H, Jaffe R (2010) Optical characterization of dissolved organic matter in tropical rivers of the Guayana Shield, Venezuela. J Geophys Res Biogeosci 115:1–15
Yamashita Y, Kloeppel BD, Knoepp J, Zausen GL, Jaffe R (2011) Effects of watershed history on dissolved organic matter characteristics in headwater streams. Ecosystems 14:1110–1122
Zeglin LH (2015) Stream microbial diversity in response to environmental changes: review and synthesis of existing research. Front Microbiol. https://doi.org/10.3389/fmicb.2015.00454

Publisher's Note Springer Nature remains neutral with regard to jurisdictional claims in published maps and institutional affiliations.